Indonesian Journal of Science & Technology

Journal homepage: http://ejournal.upi.edu/index.php/ijost/

A novel In-situ Enzymatic Cleaning Method for Reducing Membrane Fouling in Membrane Bioreactors (MBRs)

*M.R. Bilad[1,4], M. Baten[1], A. Pollet[2], C. Courtin[2], J. Wouters[3], T. Verbiest[3], and Ivo F.J. Vankelecom[1,]**

[1]Centre for Surface Chemistry and Catalysis, Faculty of Bioscience Engineering, Katholieke Universiteit Leuven, Kasteelpark Arenberg 23, Box 2461, 3001 Leuven, Belgium

[2]Laboratory of Food Chemistry and Biochemistry, Katholieke Universiteit Leuven, Kasteelpark Arenberg 20 – bus 2463, B-3001 Leuven, Belgium

[3]Department of Chemistry, K.U. Leuven and Institute of Nanoscale Physics and Chemistry (INPAC), Celestijnenlaan 200D, 3001 Heverlee, Belgium

[4]Singapore Membrane Technology Centre, Nanyang Environment and Water Research Institute, Nanyang Technological University, Singapore 637141, Singapore

*Corresponding author: Email: ivo.vankelecom@biw.kuleuven.be; Tel.: +32 16 321594; Fax: +32 16 321998

ABSTRACTS

A novel in-situ enzymatic cleaning method was developed for fouling control in membrane bioreactors (MBRs). It is achieved by bringing the required enzymes near the membrane surface by pulling the enzymes to a magnetic membrane (MM) surface by means of magnetic forces, exactly where the cleaning is required. To achieve this, the enzyme was coupled to a magnetic nanoparticle (MNP) and the membrane it self was loaded with MNP. The magnetic activity was turned by means of an external permanent magnet. The effectiveness of concept was tested in a submerged membrane filtration using the model enzyme-substrate of Bacillus subitilis xylanase-arabinoxylan. The MM had almost similar properties compared to the unloaded ones, except for its well distributed MNPs. The enzyme was stable during coupling conditions and the presence of coupling could be detected using a high-performance anion-exchange chromatography (HPAEC) analysis and Fourier transform infrared spectroscopy (FTIR). The system facilitated an in-situ enzymatic cleaning and could be effectively applied for control fouling in membrane bioreactors (MBRs).

ARTICLE INFO

Article History:
Received 2 Jan 2016
Revised 18 Feb 2016
Accepted 23 Feb 2016
Available online 29 Mar 2016

Keyword:
Membrane bioreactor (MBR)
Fouling
Magnetic membrane
Magnetic nanoparticle
In-situ membrane cleaning
Enzyme immobilisation

1. INTRODUCTION

Membrane bioreactors (MBRs) can be broadly defined as systems that integrate a conventional activated sludge system with a membrane filtration. (Judd, 2003, Visvanathan *et al.*, 2000). MBR offers a better effluent quality and a more robust technology. MBRs have thus become widely accepted as an advanced wastewater treatment option. However, its widespread application is still restricted by a membrane fouling phenomenon, which lowers the applied flux, reduces the sustainability of operation, increases the frequency of maintenance and intensive cleaning, reduces the membrane lifetime, and eventually increases the investment and operational cost. The traditional approaches for fouling control are mainly based on the physico-chemical principles, such as membrane modification, optimization of operational conditions, coagulant addition, cyclic filtration, etc, (Le-Clech *et al.*, 2006, Yeon *et al.*, 2009a, Meng *et al.*, 2009) which may not be effective and less energy efficient. Tackling the fouling remains one of the major challenges to expand its application and significantly improve its general acceptance by industries.

Figure 1 shows the mechanism and the occurence of TMP jump. In general, there are three stages of fouling (Zhang *et al.*, 2006), which are initial short-term rapid rise in TMP (stage 1 in **Figure 1**), a long-term weak rise in TMP (stage 2), followed by a TMP jump (stage 3). The occurrence of the TMP jump has been explained by several mechanisms: an increment of local flux exceeding the critical flux (CF) (Cho & Fane, 2002), a sudden change of biofilm or cake structure (Zhang *et al.*, 2006), a sudden increase in the concentration of EPS at the bottom of the cake layer (Hwang *et al.*, 2008), or the presence of N-acyl home serine lactone (AHL) as an association to biofilm formation (Yeon *et al.*, 2009a). If this is critical time when the TMP starts to jump accursed, an interruption of the filtration will occur. The overall goal of fouling control is thus to retard the occurrence of the TMP jump. (Meng *et al.*, 2009).

Activated sludge behaves as a complex and dynamic system: the TMP jump mechanisms are diverse and may in fact all occur simultaneously. The cake layer formation is initiated from the attachment of biopolymers, which starts to occur in the first stage and evolves and propagates in the second stage (See **Figure 1**). At the end of the second stage, when the local flux approaches the CF, the cake layer structure changes and an increase of EPS occur. Therefore, stage 2 plays a very important role in the occurrence of TMP Jump. More detailed investigation and properly handling of this stage can be the key step for the fouling control.

It has been widely accepted that the major fouling contributor is a cake layer that forms on the membrane surfaces (Chu & Li, 2006; Wang *et al.*, 2007; Meng & Yang, 2007; Ramesh *et al.*, 2007). This cake is formed from deposited biopolymers, which further allows easier and accelerated bacterial adhesions and holds the microbial flock on the membrane surface. A part of this cake reversibly detaches due to back-transport but the remaining cells multiply and excrete microbial products, which eventually clog the pores and form a strongly attached and irremovable fouling layer (Herzberg *et al.*, 2009). The deposited biopolymers consist of dissolved and colloidal extra-cellular polymeric substances (EPS) and soluble microbial products (SMP) (Wang *et al.*, 2008). EPS and SMP are produced by the microorganisms; they consist of a whole group of macromolecules, such as polysaccharides, proteins, nucleic acids, (phospho-)lipids, and other polymeric compounds (Le-Clech *et al.*, 2006). These compounds facilitate bacterial attachment to membrane surface and act as a shelter to

DOI: http://dx.doi.org/10.17509/ijost.v1i1
p- ISSN 2528-1410 e- ISSN 2527-8045

protect the bacteria in the biofilm-EPS matrix. EPS/SMP can be hydrolyzed by some specific enzymes, indicating an advanced way to control membrane fouling. Extracellular proteins and polysaccharides (as the main building blocks of EPS) can be degraded by proteolitic enzymes as has been successfully used for biofilm detachment (Loiselle & Anderson, 2003). In fact, enzymatic cleaning has long been applied for an intensive cleaning of fouled membranes (Maartens *et al.*, 1996). Recent studies by Yeon *et al.* showed the effectiveness of quorum quenching enzyme (acylase) coupled onto magnetic nanoparticles for preventing the formation of biofilm in MBR (Yeon *et al.*, 2009).

These results enable us to hypothesize that, in principle, membrane fouling originating from cake layer formation could also be alleviated through interrupting the initiation stage by enzymatic disruption of biopolymers. To achieve this goal, the concept of a novel in-situ enzymatic cleaning method called "magnetic enzyme-magnetic membrane" (MEMM) is introduced and evaluated in this study.

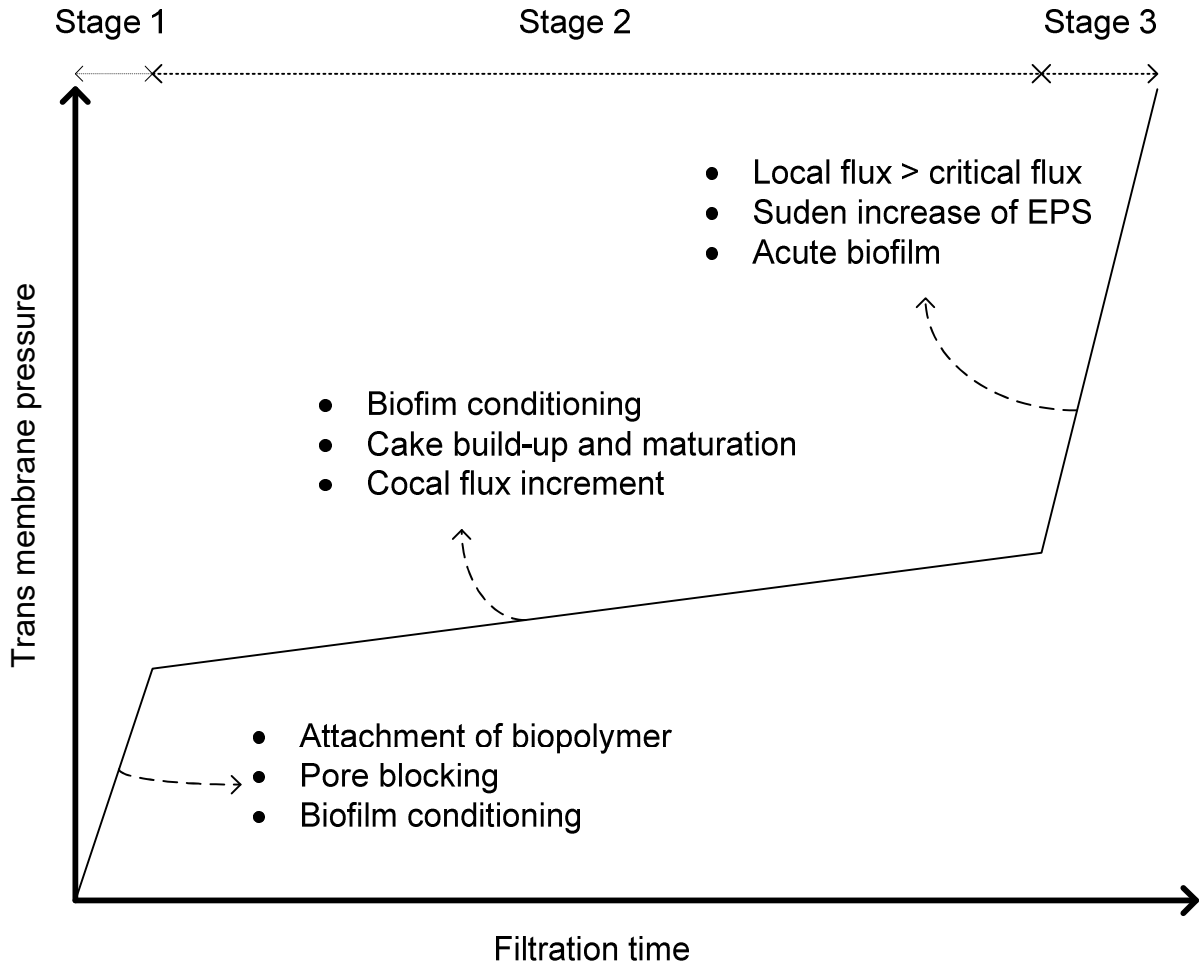

Figure 1. The mechanism and the occurrence of TMP jump.

DOI: http://dx.doi.org/10.17509/ijost.v1i1
p-ISSN 2528-1410 e-ISSN 2527-8045

In the MEMM system, the enzymes are coupled to a super paramagnetic nanoparticle to form the magnetic enzyme (ME), while the membrane is loaded with super paramagnetic nanoparticles (magnetic membrane, MM). When an external magnetic field is applied to the superparamagnetic nanoparticles, they tend to align along the magnetic field, leading to a net magnetization. In that way, applying a magnetic field to the membrane will facilitate the attraction of the ME onto the MM surface by simple magnetic attraction. The MEs are then expected to break down the foulants locally, precisely where it is needed (not in the bulk sludge solution but only on the membrane surface). Importantly, the ME can be easily released from the membrane surface by switching-off the magnet in a later stage when for instance an additional chemical cleaning of MM is required. This will prevent the destruction of the MEs by the aggressive chemical cleaning agents. After the intensive membrane cleaning, the MEs can be re-attracted to the MMs by simply reactivating the magnetic attraction. Since the MEMM operates very locally, the necessary amount of enzyme is expected to be much lower. As the cleaning process occurred continuously throughout the operation, this could be a more direct approach for fouling control in MBRs. This approach is non-toxic, environmentally benign and highly specific compared to aggressive chemicals that may also oxidize the membrane (Puspitasari & Liany, 2009) to shorten the membrane life span and damage the environment.

To prove the effectiveness of this novel MEMM concept, a model arabinoxylane substrate was used together with endo-β-1,4-D-xylanase. To achieve this objective, the research was conducted by the following steps:

(1) Preparation of magnetic nanoparticles (MNP) that exhibit super paramagnetic properties,

(2) Preparation and characterization of MM and evaluation of their magnetic properties,

(3) Characterization of the fresh enzyme,

(4) Preparation of ME and optimization of the immobilization process,

(5) Performance evaluation or system tests.

2. MATERIALS AND METHODS

2.1. Membrane preparation and module potting

The flat sheet membranes were prepared from polysulfone (PSF) (BASF-Ultrason)/N-Methyl-2-pyrrolidone (NMP) (ACROS) solutions (12, 14 and 16%) by phase inversion (Vankelecom *et al.*, 2004). The polymer solutions were cast with a 250 µm wet thickness of casting knife on a polypropylene support (Novatexx 2471, kindly supplied by Freudenberg, Germany) and casting speed of 2.25 cm/s. The casting was performed in a semi-closed hood at ambient temperature (18-20°C) and a relative humidity of 20-30%. The casted polymer solution was immediately immersed into a coagulation bath containing demineralized water as non-solvent. Afterwards, the membrane was immediately stored in tap water prior to be used. To prepare MM, a series of 12% of PSF/NMP solutions were added with 10%, 20% and 30% (%w) of MNP. The relatively high MNP concentrations were chosen to obtain sufficient magnetic attraction force. To prevent MNP aggregation, the solvent was divided into two parts: (i) to dissolve the polymer (polymer solution) and (ii) to dissolve the MNP (MNP solution). The MNP solution was placed into a sonification device for four hours to break the aggregation. Subsequently, the polymer and MNP solutions were mixed and immediately stirred by using a mechanical stirrer and

DOI: http://dx.doi.org/10.17509/ijost.v1i1
p- ISSN 2528-1410 e- ISSN 2527-8045

sonificated just before casting. Prior to use in system test, the MM was potted according to our previous reference (Bilad *et al.*, 2010).

2.2. Super paramagnetic nanoparticle (MNP) preparation

The preparation of MNP was conducted in the Institute for Nanoscale Physics and Chemistry (INPAC), Molecular and Nanomaterials, Katholieke Universiteit Leuven. All chemicals were analytical grade, and they were used as received. The materials used for MNP preparation were ethylene glycol, octylamine, iron(III) chloride ($FeCl_3$), demineralized water (H_2O), hydrogen chloride (HCl), and xylene (3-(bis(2-hydroxyethyl)amino)prophyl-triethoxysilane). To synthesize approximately 100 mg of MNP, 37.5 mL of ethylene glycol and 37.5 mL of octylamine were first mixed in a reactor placed in an oil bath at 140°C and added with a mixture of 2.4 g of iron chloride, 10 mL of octylamine and 4 mL of distilled water (mixed at 50°C) by using a pipette. When the solution started to evaporate, the temperature was increased to 175°C, and until then the reflux was captured and kept for 24 hours. The color of the solution changed from brown to black, indicating the formation of MNP. To separate MNP from the solution, the solution was poured into a beaker glass and was added with acetone (act as non solvent for MNP). By placing a magnet at the outside-bottom of the beaker glass, the MNP settled at the bottom. The MNP were separated from the liquid phase by decantation. This procedure was repeated several times followed by vacuum dried at room temperature to obtain dry MNP powder. The hydrophilization of the MNP was done by addition of 1 mL of xylene (3-(bis(2-hydroxyethyl)amino)prophyl-triethoxysilane) and few drops of acetic acid in MNP/acetone solution (±100 mL). This solution was sonicated for one hour to break the MNP aggregate following by the addition of distilled water until two phases solution were formed (the hydrophilic MNP moved to the water phase), which eventually could be separated by decantation. The MNP were recovered by vacuum drying. The MNP have a typical size of approximately 15±5 nm with difference ratios of acid to hydroxyl groups (0.001, 0.01, 0.05 and 0.1) obtained from further treatments.

2.3. Enzyme, substrate, and enzyme characterization

The model enzyme used in this study was Endo-β-1,4-D-xylanases (BsXynA) (EC 3.2.1.8). The further characterics of the enzyme were given by references (Vandermarliere *et al.*, 2008; Pollet, 2010). The BsXynA was prepared in Laboratory of Food Chemistry and Biochemistry and Leuven Food Science and Nutrition Research Centre (LFoRCe), Katholieke Universiteit Leuven. The substrate of BsXynA used in this study was arabinoxylan.

(1) Determination of the pH optimum

The pH optimum of BsXynA was determined by measuring enzyme activities at different pH levels. The xylazyme tablet (substrate) was placed into the tubes containing different buffer solutions: sodium acetate (NaOAc) buffers at pH 3, 4, and 5; sodium phosphate (Na_2HPO_4)/sodium biphosphate (NaH_2PO_4) buffers at pH 6, 7 and 8 (VWR International, Belgium). The enzyme activity was measured by performing a colorimetric xylazyme activity test on the different test tubes (Section 0) contaning solution with different pH. To check the pH stability, the BsXynA was stored in different pH: 3, 4, and 5 in NaOAc buffer and pH 6, 7, and 8 in Na_2HPO_4/NaH_2PO_4 buffer for 2 hours at room temperature prior to be used. Subsequently, the pH-values were adjusted to optimal pH by diluting it in MOPS buffer (pH = 6.5; 20 mM) for relative activity tests.

DOI: http://dx.doi.org/10.17509/ijost.v1i1
p-ISSN 2528-1410 e-ISSN 2527-8045

(2) Determination of the temperature optimum and stability

The temperature optimum of BsXynA was determined by measuring the activities at its optimum pH. The reaction tubes were placed in water baths at temperatures of 20, 30, 40, 50, 60, and 70°C during the incubation. The activity of the enzyme was measured using Xyalazyme method. For temperature stability, the BsXynA was stored in different temperatures of 20, 30, 40, 50, 60, and 70°C for 40 minutes prior to be used. Subsequently, the activity of BsXynA was measured at temperature of 40°C and pH of 6.5 in a MOPS buffer (20 mM) for relative activity tests.

2.4. Coupling of BsXynA to MNP and optimization of coupling procedure

The MNP was coupled to the enzyme by covalently bind the carboxylic acid (-COOH) groups on the MNP to the amine ($-NH_2$) groups on the enzyme using N-(3-dimethylaminopropyl)-N'-ethylcarbodiimide (EDC) (Sigma-Aldrich) and N-hydroxysuccinimide (NHS) (Sigma-Aldrich) cross-linking agents. The coupling procedure consists of two steps: activation (step 1) and reaction (step 2). To obtain the maximum coupled enzyme yield, the coupling was performed in different parameters: the ratio of carboxylic acid to amine groups of: 0.1, 1, 5, 10 and 100%; ratio of enzyme to MNP (%wt/%wt) of 10, 1 and 0.1; reaction time of 2 and 24 hours; reaction buffers; and the storage solutions. All experiments were preformed in triplicate.

2.5. Experimental set-up and system test

To prove the concept of the in-situ cleaning technique, the system tests were carried out by using prepared MM and ME in lab-scale set-up. The tests were consisted of three parts: (1) Ability of magnetic attraction of ME into MM surfaces by mean of magnetic attraction in a stirred solution; (2) Investigation if ME could reduce fouling on MM in comparison with a control; and, (3) Investigation of condition if ME could be used for enzymatic cleaning of fouled membranes. The experiment set-up used for this experiment is shown in **Figure 2**.

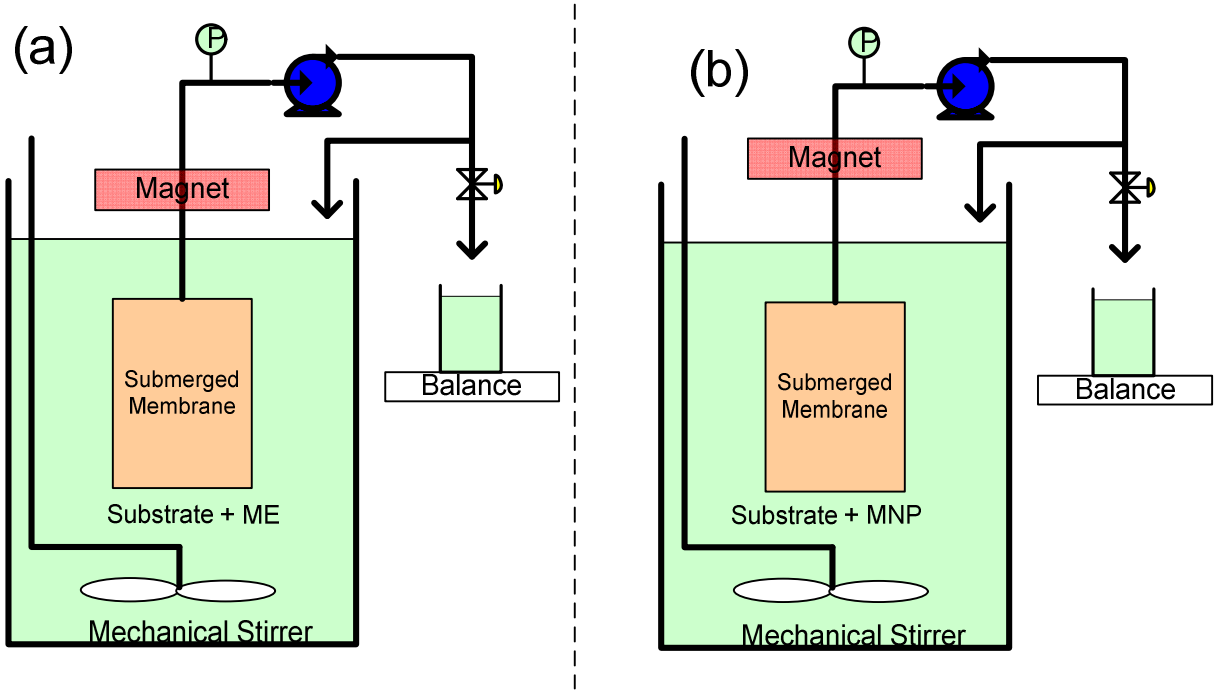

Figure 2. Experimental set-up for system test, (a) MEMM system, (b) control.

DOI: http://dx.doi.org/10.17509/ijost.v1i1
p- ISSN 2528-1410 e- ISSN 2527-8045

The ability to magnetically attraction ME into MM was tested in a continuously stirred reactor. A MM module was placed inside the reactor, which contain solution in addition of ME. The attraction of ME to MM was observed visually. To investigate the effectiveness of the system to control fouling, the ME (190 AU) was added to a bulk solution containing 1 g/L arabinoxylan. In this case, arabinoxylan acted as substrate for ME and as solute to be filtered by the membrane. Meanwhile, the control reactor contained of NP and arabinoxylan. The filtration was derived from peristaltic pump and the TMP was measured from installed manometer. To obtain a moderate TMP built-up, the filtration flux was set at 6.58 L/m^2/h, and the TMP was monitored over time (24 hours) for both the control and MEMM reactors. A mechanical stirrer was used to homogenously mix the solution. The magnetic field was derived from permanent magnet placed at top of both reactors. In the final phase, the cleaning potential of ME was also investigated. The fouled module in the control solution was brought into the reactor, which contained ME without cleaned. Meanwhile, the module in MEMM system was first physically cleaned to be sure all ME were removed from the membrane.

3. ANALYTICAL METHODS

3.1. Membrane characterization

The permeability of the membranes was determined with the 'High throughput (HT)' apparatus (Vandezande *et al.*, 2005) at constant pressure of 0.25 bar. With this device, the permeability of 16 samples (2.24 cm^2) cut from membrane sheets (n=5), could be obtained simultaneously. The flux (J) and permeability (L) of the membrane was calculated by using equations (1) and (2), respectively. Equations (1) and (2) can be expressed in the following:

$$J = \frac{V}{A\,t} \quad (1)$$

$$L = \frac{J}{TMP} \quad (2)$$

where J is the flux (L/m^2/h), V is the volume (L), t is the time (hours), L is the permeability (L/m^2/h/bar), and TMP is the trans-membrane pressure (bar). The CWP was determined for fresh membranes without MNP and MM to compare their properties.

The microstructure of the membranes was observed using a scanning electron microscope (SEM; Philips SEM XL30 FEG with Adax dx-4i system). To obtain the thickness, the SEM images of the cross section of the membrane were visually observed and measured after breaking the membranes under a liquid nitrogen. To further analyze the presence of MNP in the MM, an elemental analysis to identify the composition of the inorganic specimen in the MM was performed by using an energy-dispersive X-ray spectroscopy (EDX) that is integrated with SEM.

3.2. Determination of the activity and activity unit

The activity of the BsXynA was determined by using the Colorimetric Xylazyme AX method according to Pollet *et al.* (Pollet, 2010; Pollet *et al.*, 2009) The absorbance was plotted as a function of enzyme concentration and extrapolated to obtain the enzyme concentration where the absorbance should equal to 1.

3.3. High-Performance Anion-Exchange Chromatography (HPAEC) with integrated Pulsed Amperometric Detection (PAD)

The presence of coupling was analyzed using high-performance anion-exchange chromatography (HPAEC) with integrated pulsed amperometric detection (PAD) according to Pollet *et al.* (Pollet *et al.*, 2009) In this test, the xylohexaose (X6) (Megazyme, Ireland) was used as a

DOI: http://dx.doi.org/10.17509/ijost.v1i1
p-ISSN 2528-1410 e-ISSN 2527-8045

substrate because it has smaller structure. The L-Rhamnose (Sigma-Aldrich, Belgium) was used as a standard solution. The smaller substrate was used to prevent steric effect due to support material that probably existing in Xylazyme AX tablets. The experiments were performed in triplicate.

3.4. Fourier Transform InfraRed (FTIR) spectroscopy

The FTIR was used to identify the presence of –CONH- bond as a covalent bridge between enzyme and MNP. The immobilization of BsXynA occurred via amine groups present on the enzyme that bind to carboxylic groups on the MNP. As a consequence, the presence of a –CONH- bond could prove the coupling of the enzyme to a MNP. Individual FTIR samples were prepared for NP and ME. Approximately 10 mg of dried NP and ME were mixed with potassium bromide (Fluka) in a proportion of 10/90 (%wt). The mixture was crushed into become powder and further pressed to form a thin transparent film.

4. RESULTS AND DISCUSSION

4.1. Membrane and magnetic membrane characteristics

The effect of polymer concentration on CWP of fresh membrane and MM are shown in **Figure 3.** The permeability of the membranes, both fresh and MM were in the range of UF to MF. It decreased with the increase of polymer concentration. For MM, the CWP slightly decreased with increasing NP concentrations, and this is only significant for 30 wt% of MNP.

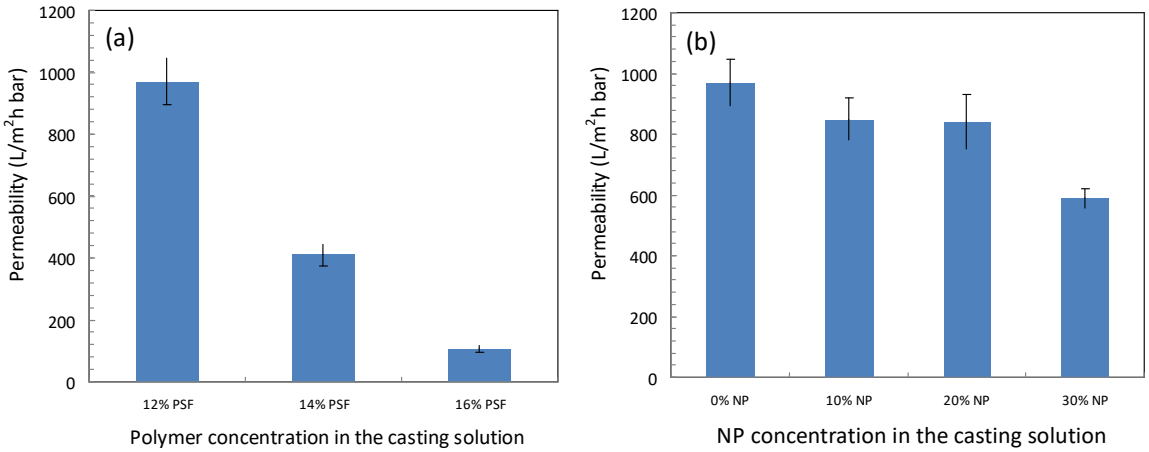

Figure 3. Permeability of (a) PSF membranes, (b) MM

The SEM images of the PSF and MM (surface and cross section) are shown in **Figure 4**. Results show that incorporation of MNP changed the membrane structure. The MM surfaces seem to be more compact in presence of MNP (20 and 30% for **Figure 4(a)** and **(b)**, respectively). The white spots are clusters of MNP embedded in the PSF polymer matrix. The cross section images of magnetic membranes also show that the MM (38 µm) is thinner than the fresh membranes (90-100 µm), even though both were cast at similar wet thickness. The presence of MNP in the MM can be observed visually from the change of color from white in fresh membranes to brown-black in MM. The magnetic properties of MM were simply tested by putting them close to a permanent magnet. The MM attracted to the permanent magnet at the distance of 1-2 cm.

DOI: http://dx.doi.org/10.17509/ijost.v1i1
p- ISSN 2528-1410 e- ISSN 2527-8045

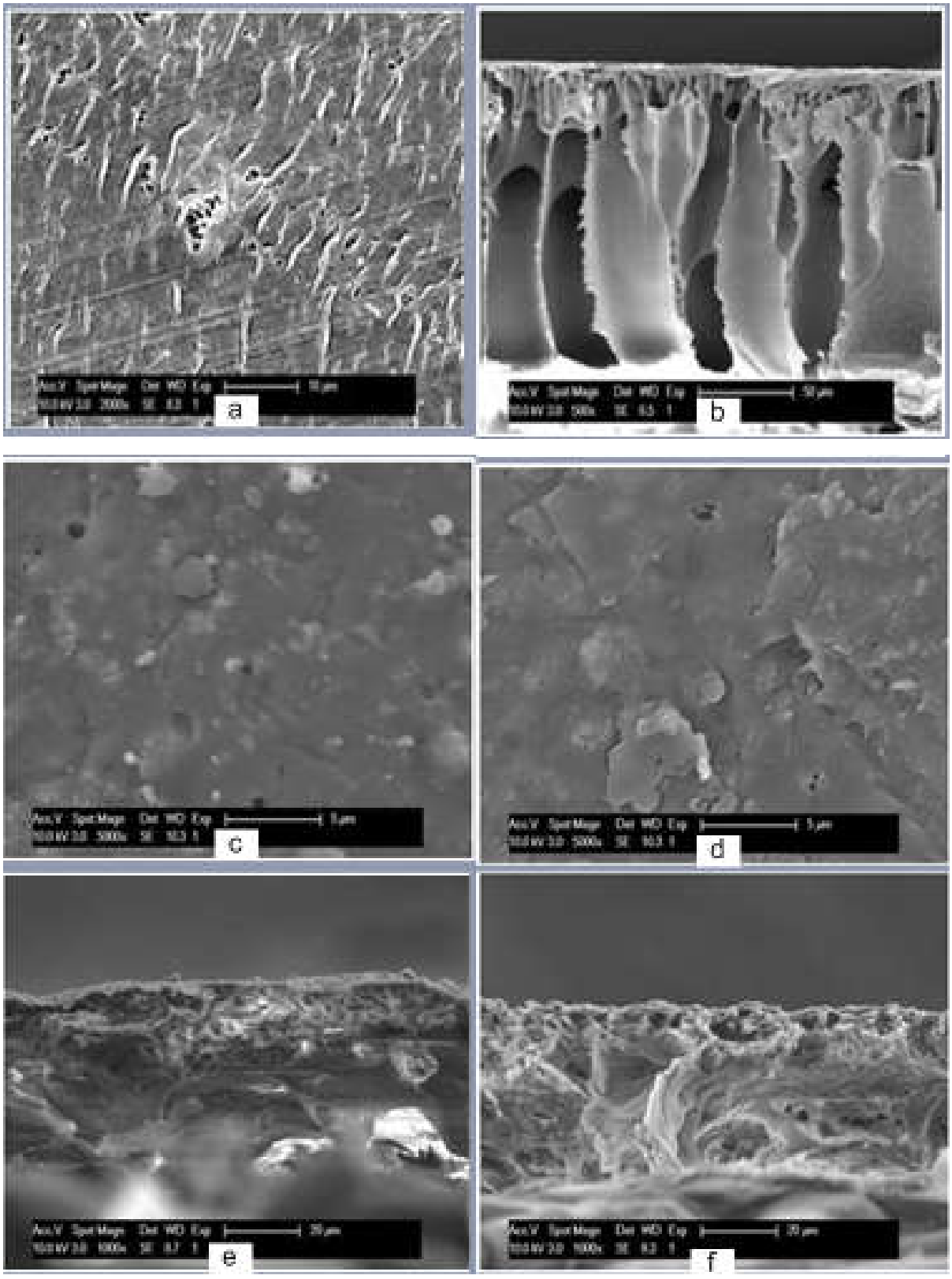

Figure 4. SEM images of membranes: a) surface of fresh membrane, b) cross section of fresh membrane, (c-d) surfaces of MM, (e-f) cross section of MM

DOI: http://dx.doi.org/10.17509/ijost.v1i1
p-ISSN 2528-1410 e-ISSN 2527-8045

The presence of MNP in the MM was further analyzed by performing an elemental analysis using EDX. The elemental analysis of the MM is shown in **Figure 5**. Three elements were clearly present and dominant in the MM, namely sulfur (S) from polymer material (PSF), calcium (Ca) from tap water used to store the membrane, and iron (Fe) from MNP.

4.2. BsXynA activity

The activity of BsXynA was able to be measured using Colorimetric Xylazyme AX method (See **Figure 6**). Acording to the test, one XU was corresponded to 0.088 µg/mL of BsXynA. This value would be used to compare activities in the following experiments under different conditions. To obtain the optimum pH of BsXynA, relative activity of BsXynA was checked at different incubating pH as plotted in **Figure 6(a)**. The highest activity was found at a pH of 6-7. Only less than 40% activity could be maintained when the incubation at pH between 5 and 8. The stability of the enzyme after an expose to different buffer solution for two hours, is shown in **Figure 6(b)**. The relative activity of enzyme changed when it was stored not at their optimum pH. The loss of activity was tolerable for a pH range of 4 to 8 with less than 20% activity loss. However, too acidic or alkaline solutions could significantly reduce its activity. For instance, at pH 3, the enzyme lost 50% of its activity.

The relative activity of BsXynA at different temperatures is shown in **Figure 6(c)**. The highest activity was found at 40 °C. Total loss of activity was found at 60°C and up to 80% loss when the reaction temperature down to 20°C. To explore the allowable range of enzyme storage temperature and coupling condition, the stability of enzyme after stored at different temperatures for 40 minutes was tested. The effect of storage temperature on enzyme activity is shown in **Figure 6(d)**. BsXynA was relatively stable at a temperature below 40°C. However, above it, significant activity loss was found. An increasing of temperature to above 50°C leads enzyme denaturation, resulting in a total loss of its activity. Further experiments for activity measurement were carried out in MOPS buffers (20 mM) (or McIlvaine buffer) at a pH of 6.5 and incubation temperature of 40°C.

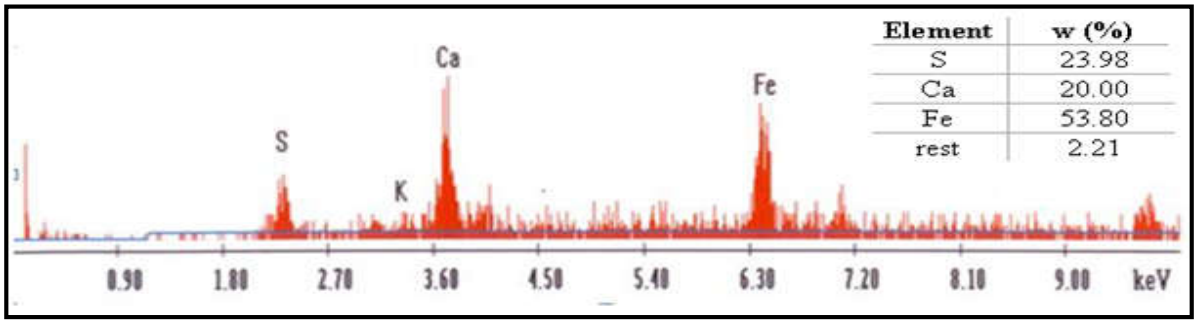

Figure 5. Elemental analysis of MM

DOI: http://dx.doi.org/10.17509/ijost.v1i1
p- ISSN 2528-1410 e- ISSN 2527-8045

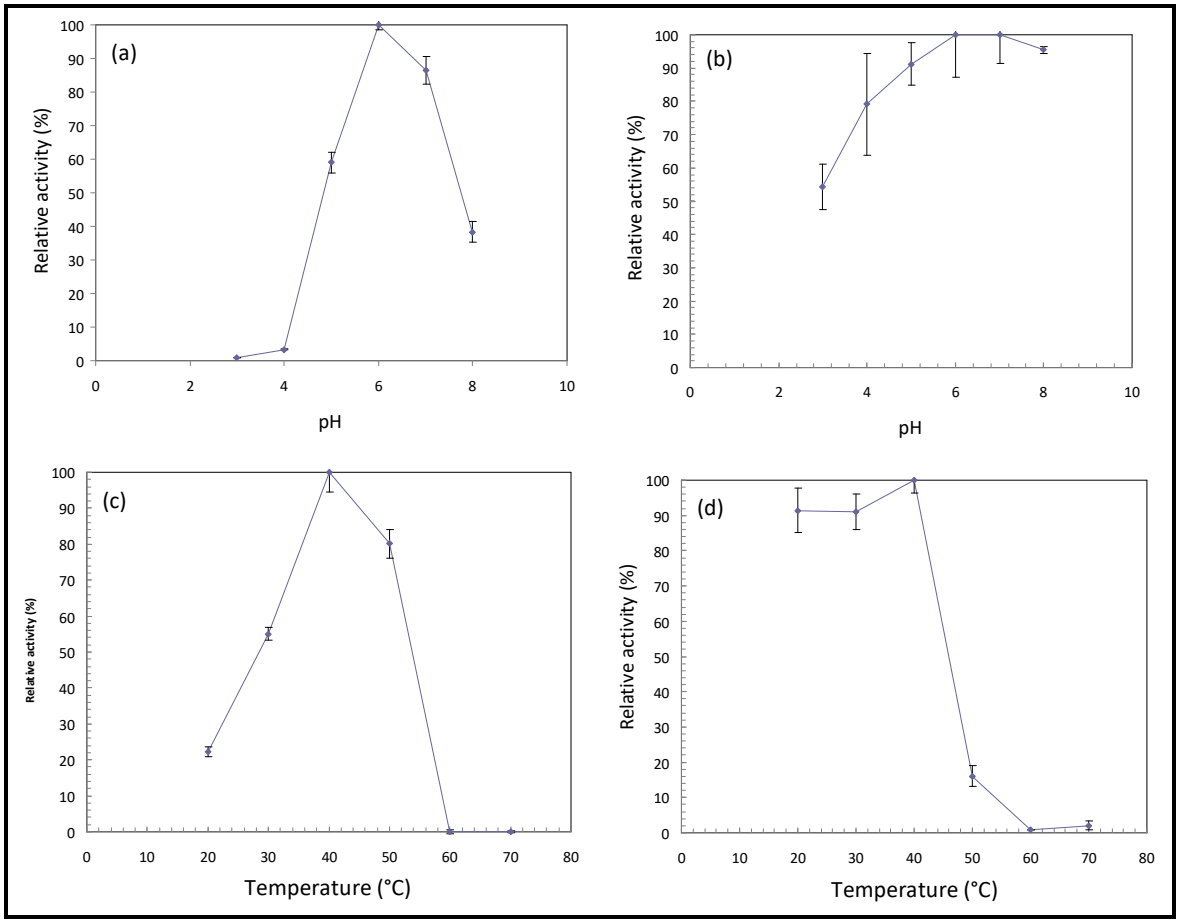

Figure 6. Relative activities of BsXynA: (a) at different pH of reaction, (b) after storage for 2 hour at different buffers, (c) at different temperatures of reaction, (b) after storage for 40 minutes at different temperatures.

4.3. Coupling analysis and effect of coupling parameters

4.3.1. Coupling analysis

The effectiveness of coupling of BsXynA into MNP using EDC/NHS as cross linking agent was observed using two methods: FTIR and HPAEC-PAD. The absorbance spectra of ME and NP from FTIR analysis are shown in **Figure 7.** The peaks below 1500 cm-1 represent organic content of the enzyme. The presence of carboxylic groups in NP and MEC was proven by spectras at wavelengths of 3000 – 2500 cm-1. As prove of coupling, the presence of the –CONH- bond is most important to see from the spectra. This bond is located in wavelengths of 1680 – 1630 cm-1 and highlighted in **Figure 7.** The ME absorbance showed two peaks around 1669 and 1649 cm-1 which correspond to the presence of the -CONH- bond which prove the coupling of enzyme to MNP.

The ME made from MNP with 10% acid groups and enzyme/MNP ratio of 0.1 to 1 was used as sample for HPAEC-PAD analysis. The chromatograms of the hydrolysis products produced from wild type xylanse and the ME are shown in **Figure 8(a)** and **(b)**. It is clear that xylohexaose was mainly cut into xylotriose both for wild type xylanse and the ME. Result indicates that ME was contained with BsXynA which eventually broke down xylohexaose into xylotriose as shown in **Figure 8(b).**

DOI: http://dx.doi.org/10.17509/ijost.v1i1
p-ISSN 2528-1410 e-ISSN 2527-8045

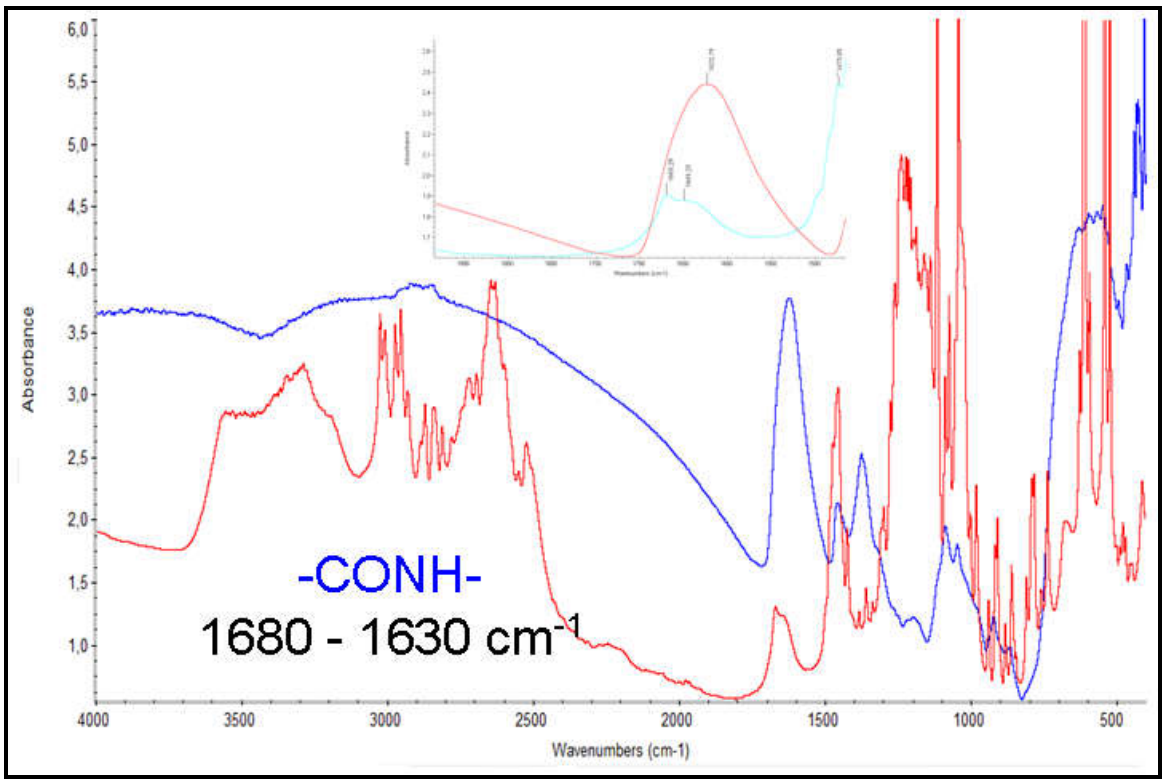

Figure 7. Absorbance spectra of NP and ME

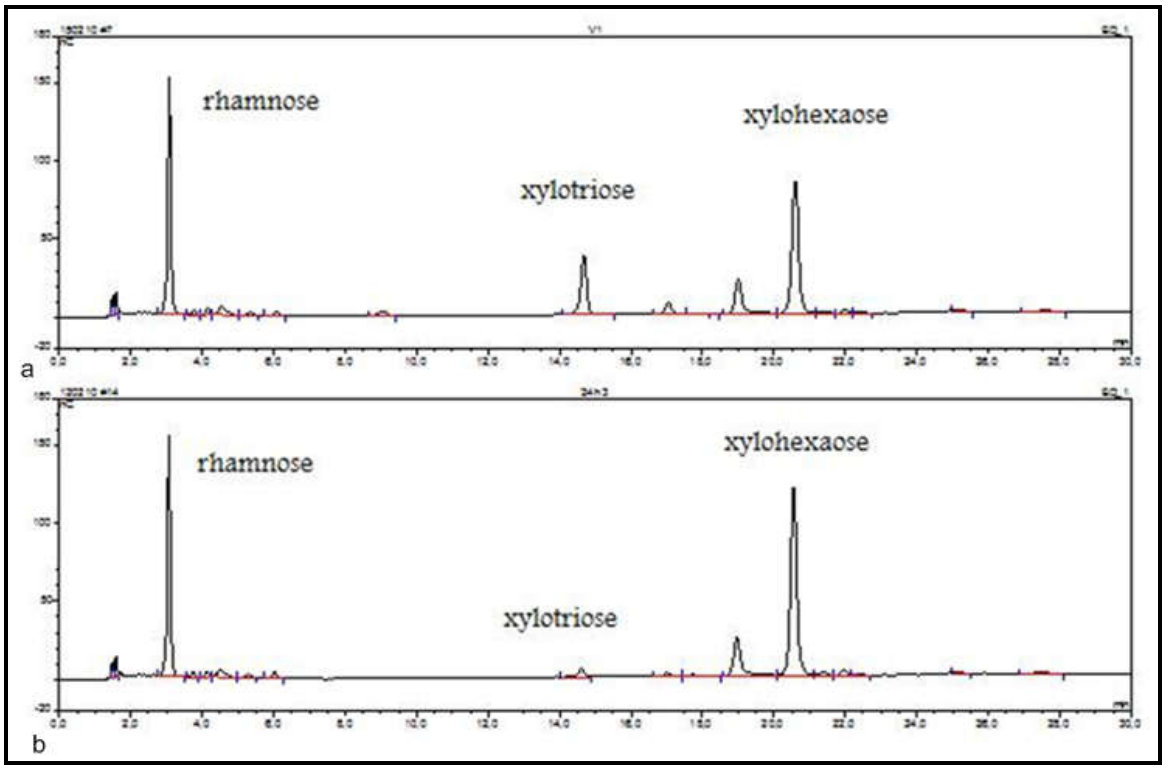

Figure 8. Chromatogram of the hydrolysis products produced after incubation of X6: (a) BsXynA and (b) ME.

DOI: http://dx.doi.org/10.17509/ijost.v1i1
p- ISSN 2528-1410 e- ISSN 2527-8045

4.3.2. Coupling optimization

The surface area of peaks on the chromatograms from HPAEC-PAD analysis is correspond to the enzyme activity. Comparison of wild type xylanse to ME shows of only 0.583% of free enzyme activity can be maintained after the coupling process. The analysis using Colorimetric Xylazyme AX method was also found in similar magnitude. This could be due to loss of activity during the coupling process or due to low efficiency of coupling. To obtain high activity yield on the ME, a series of coupling with different operational parameters were performed to optimize the coupling: (1) percentage of acid groups on the MNP, (2) the ratio of enzyme to MNP, (3) cross-linking reaction time (step 2), (4) different buffers in the activation step (step 1) and reaction step (step 2) and (5) storage of MEC in different buffers. For coupling optimization, the activity was measured using Colorimetric Xylazyme AX method.

4.3.2.1. Effect of the ratio of acid group on hydroxyl group on the MNP

A series of coupling with different acid groups on MNP (0.1%, 1%, 5%, 10% and 100%) were performed using enzyme to NP ratio: 0.1 mg of enzyme/mg NP, 2 hours of reaction time. The activity of ME and the activity of uncoupled enzymes left in the supernatant were measured and the results are shown in **Figures 9(a)** and **(b).** The activity of ME and supernatant are represented as their relative activity compared to the initial amount of activity of BsXynA added to perform the coupling. Results show that ME formed from MNP with 10% of acid group has the highest activity. This MNP was used for further tests.

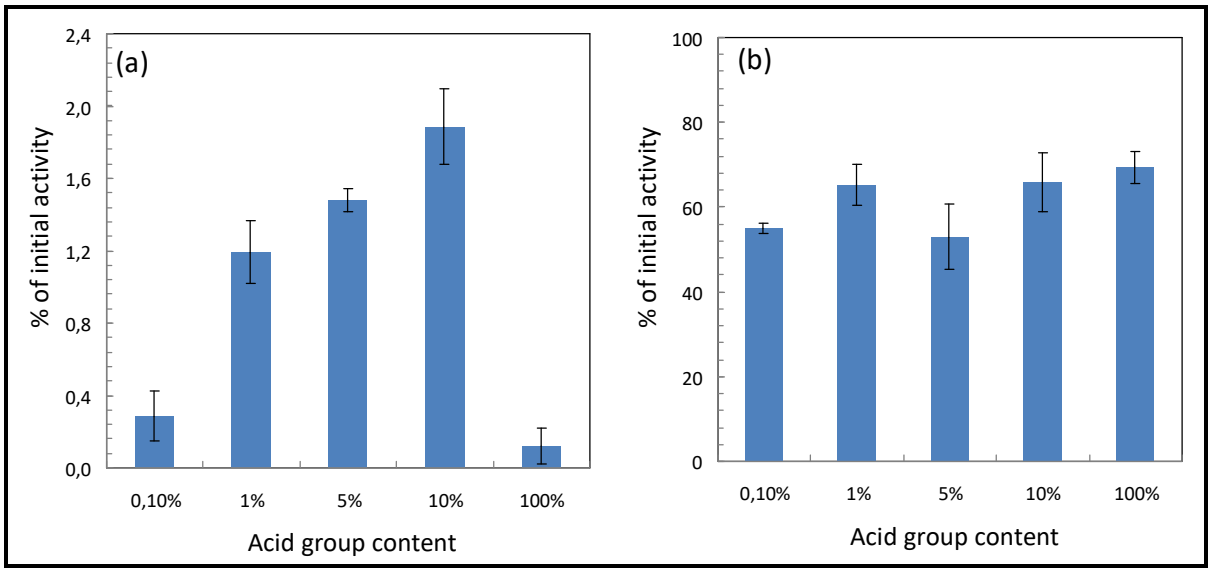

Figure 9. The activity of (a) ME and (b) non-coupled enzyme residue in supernatant for MNP with different percentages of acid groups. Notice the different scale of y-axis.

DOI: http://dx.doi.org/10.17509/ijost.v1i1
p-ISSN 2528-1410 e-ISSN 2527-8045

4.3.2.2. *Effect of the enzyme/MNP ratio*

Figure 10 shows the activity of ME and non-coupled enzyme residue in supernatant for MNP with different percentages of acid groups. In the figure, the different scale of y-axis must be considered. In the experimental procedure, the coupling of enzyme to MNP was performed with three different enzyme/MNP ratios of 0.1, 1, and 10 and 2 hour coupling reaction. The activity of ME and the activity of uncoupled enzymes left in the supernatant are shown in **Figures 10(a)** and **(b).** The highest activity was found for enzyme/MNP ratios of 0.1. This ratio was used for further tests.

4.3.2.3. *Effect of reaction time*

To investigate the effect of the coupling reaction time (step 2), the coupling of enzyme to MNP were performed for 2 and 24 hours. The activity of coupled enzymes (ME) and the activity of uncoupled enzymes left in the supernatant are shown in **Figures 11(a)** and **(b)**. The reaction times did not have a significant influence on the coupling efficiency of ME. The lower activity for longer reaction duration was probably due to longer storage time at room temperature during the reaction. The reaction time of 2 hours was used for further tests.

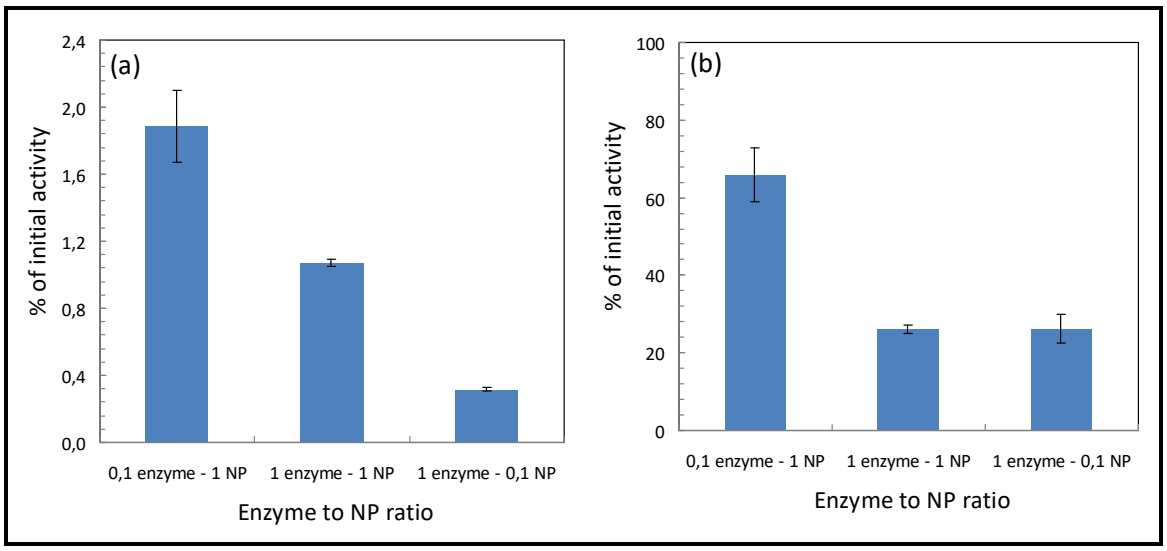

Figure 10. The activity of (a) ME and (b) non-coupled enzyme residue in supernatant for MNP with different ratio of enzyme/MNP. Notice the different scale of y-axis.

DOI: http://dx.doi.org/10.17509/ijost.v1i1
p- ISSN 2528-1410 e- ISSN 2527-8045

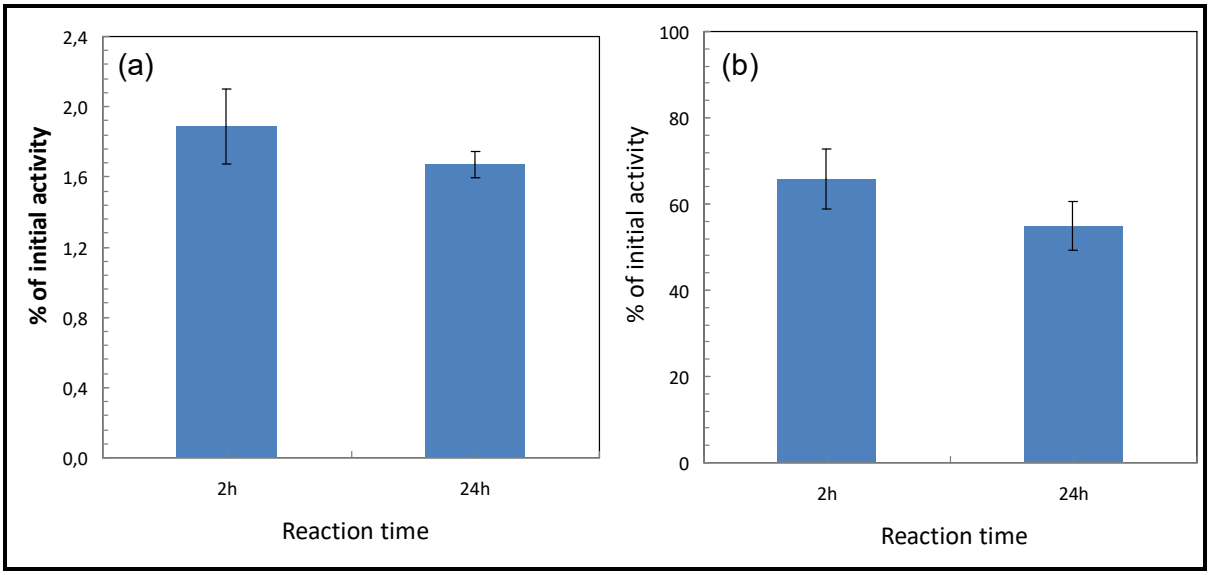

Figure 11. The activity of (a) ME and (b) non-coupled enzyme residue in supernatant with different coupling reaction times. Notice the different scale of y-axis

4.3.2.4. *Effect of different buffers in the activation step (step 1) and reaction step (step 2)*

Figure 12 shows the activity of ME and non-coupled enzyme residue in supernatant with different buffer conditions in coupling steps. The effect of different buffer solutions in step 1 and 2 of the EDC/NHS coupling procedure was examined. All optimized parameters from previous test were used in this test, except that activity was measured in McIlvaine buffer instead of MOPS buffer.

The activity of ME and supernatant are shown in **Figures 12(a)** and **(b).** The highest immobilization obtained based on activity measurements was for a combination of H_2O in steps 1 and 2 in addition of few drops acetic acid at step 1. The coupling efficiency of 1.2% was obtained.

4.3.2.5. The effect of storage of MEC in MOPS buffer versus McIlvaine buffer

The effect of ME storage buffer after coupling was observed in this test. The ME was prepared according to the all optimum parameters obtained from previous tests. The activity of ME was compared for storage in McIlvaine or MOPS buffer. The relative activity of ME and supernatant in different storage solutions are shown in **Figure 13(a)** and **(b)**. Results show that the activity of ME was higher when stored in MOPS (8.3%) compared to McIlvaine buffer (1.2%). The difference in residual activity is probably due to different separation efficiency. The ME seem to be more dissolve in McIlvaine than in MOPS buffer. McIlvaine buffer has good interaction with ME and keep ME remain in suspension. This is also confirmed by the residual activity measured in the supernatant of MOPS (26.1%) and McIlvaine (46.0%) buffer. The ME that present in McIlvaine, were probably wash-out with the supernatant in washing step due to a poor magnetic settling separation.

DOI: http://dx.doi.org/10.17509/ijost.v1i1
p-ISSN 2528-1410 e-ISSN 2527-8045

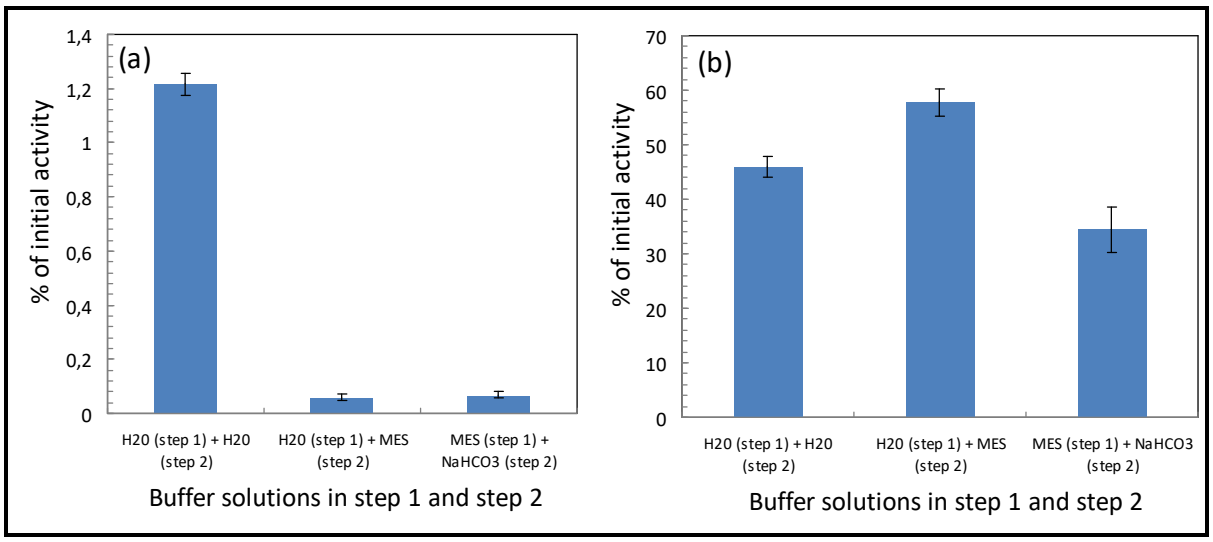

Figure 12. The activity of (a) ME and (b) non-coupled enzyme residue in supernatant with different buffer conditions in coupling steps. Notice the different scale of y-axis

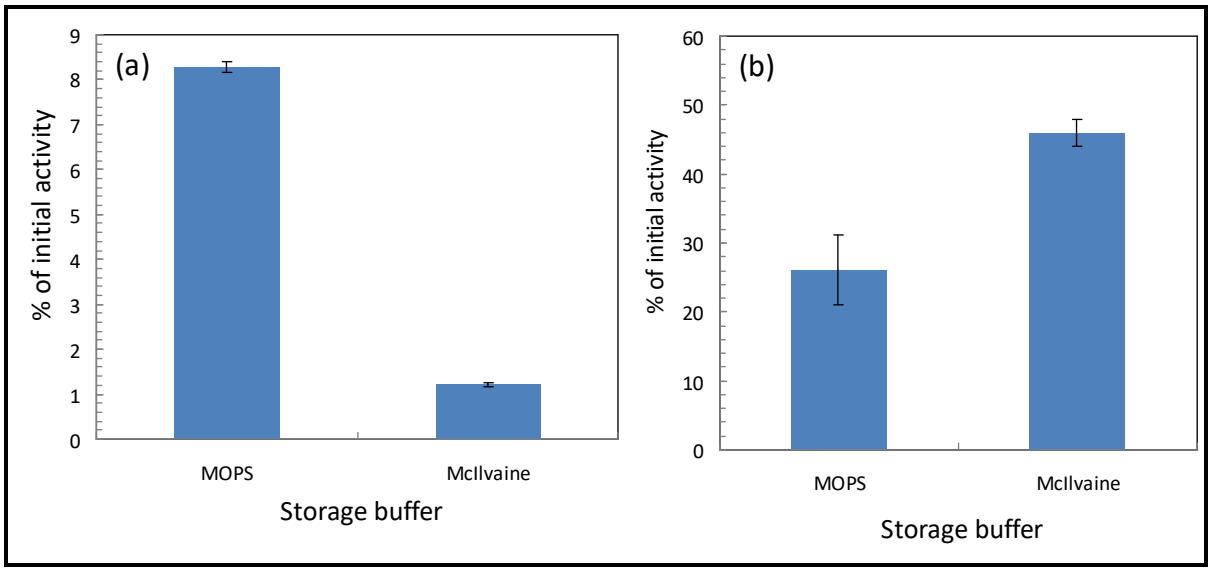

Figure 13. The activity of (a) ME and (b) non-coupled enzyme residue in supernatant with different storage buffer. Notice the different scale of y-axis

DOI: http://dx.doi.org/10.17509/ijost.v1i1
p- ISSN 2528-1410 e- ISSN 2527-8045

4.3.3. Performance of ME-MM in filtration system

4.3.3.1. Magnetic attraction and MNP recovery

The preliminary system test was conducted to evaluate the ability of a super paramagnetic material (in this case, weak iron) to magnetically attract ME from a well-mixed-bulk solution. In this case, weak-iron mimicked the function of MM. The result of the system test is shown in **Figure 14.** When the system induced with magnetic field by placing the permanent magnet close to the weak iron, the suspended ME was attracted into the surface of weak-iron. However, the ME were not distributed homogeneously over the surface. This is because of magnetic strength distribution. This phenomenom is a typical characteristic of magnetic materials. They posses stronger magnetic properties on their edges than in the middle. However, the test using MM module revealed that the ME was attracted well distributedly, since MNP were distributed into the polymer membrane matrixes (pictures not shown). This first phase of the system test proved that ME could effectively be magnetically attracted onto a super paramagnetic surface.

4.3.3.2. Fouling reduction potential of ME

The fouling reduction potential by means of in-situ enzymatic cleaning of membranes was investigated in a dead-end filtration system. The MM was potted into two small envelopes which have an effective filtration area of 2 x (4 x 8) cm2. One membrane was used in presence of ME and the other as a control in presence of MNP. The TMP profile of the filtration is shown in **Figure 15.**

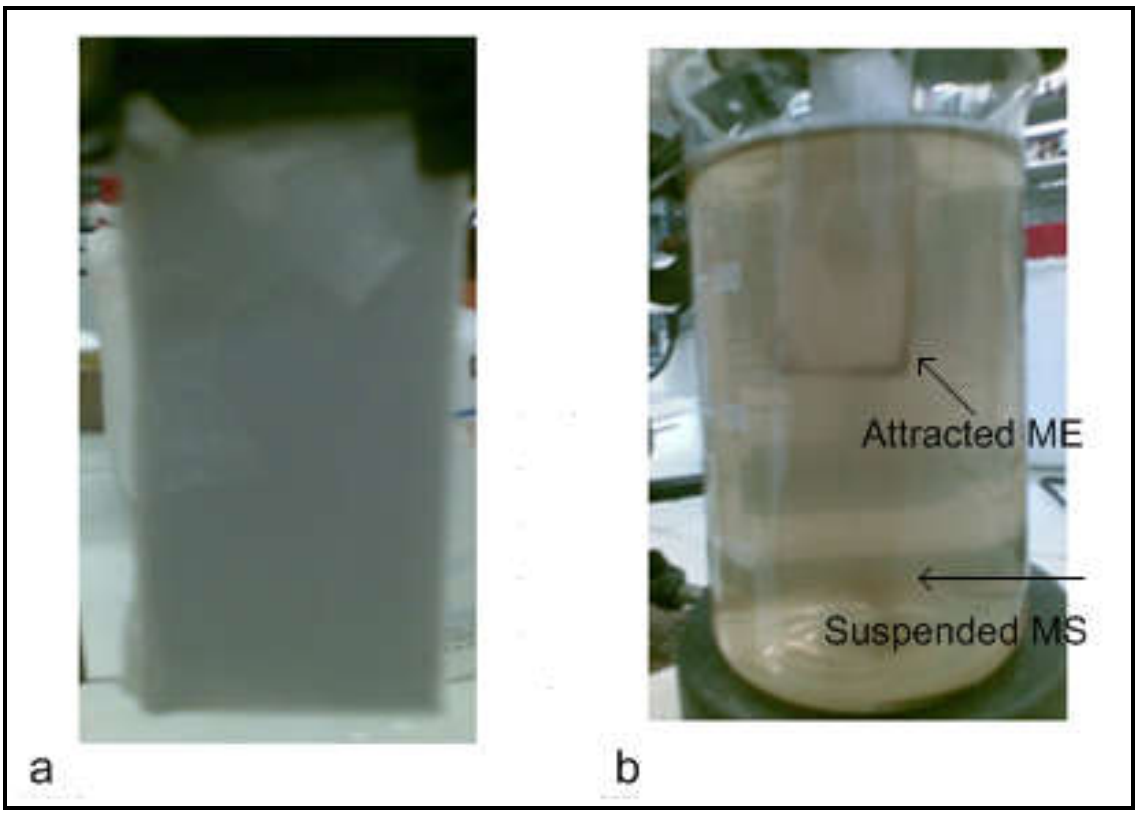

Figure 14. Magnetic surface before (a) and after (b) immersion in a water solution containing suspended ME.

DOI: http://dx.doi.org/10.17509/ijost.v1i1
p-ISSN 2528-1410 e-ISSN 2527-8045

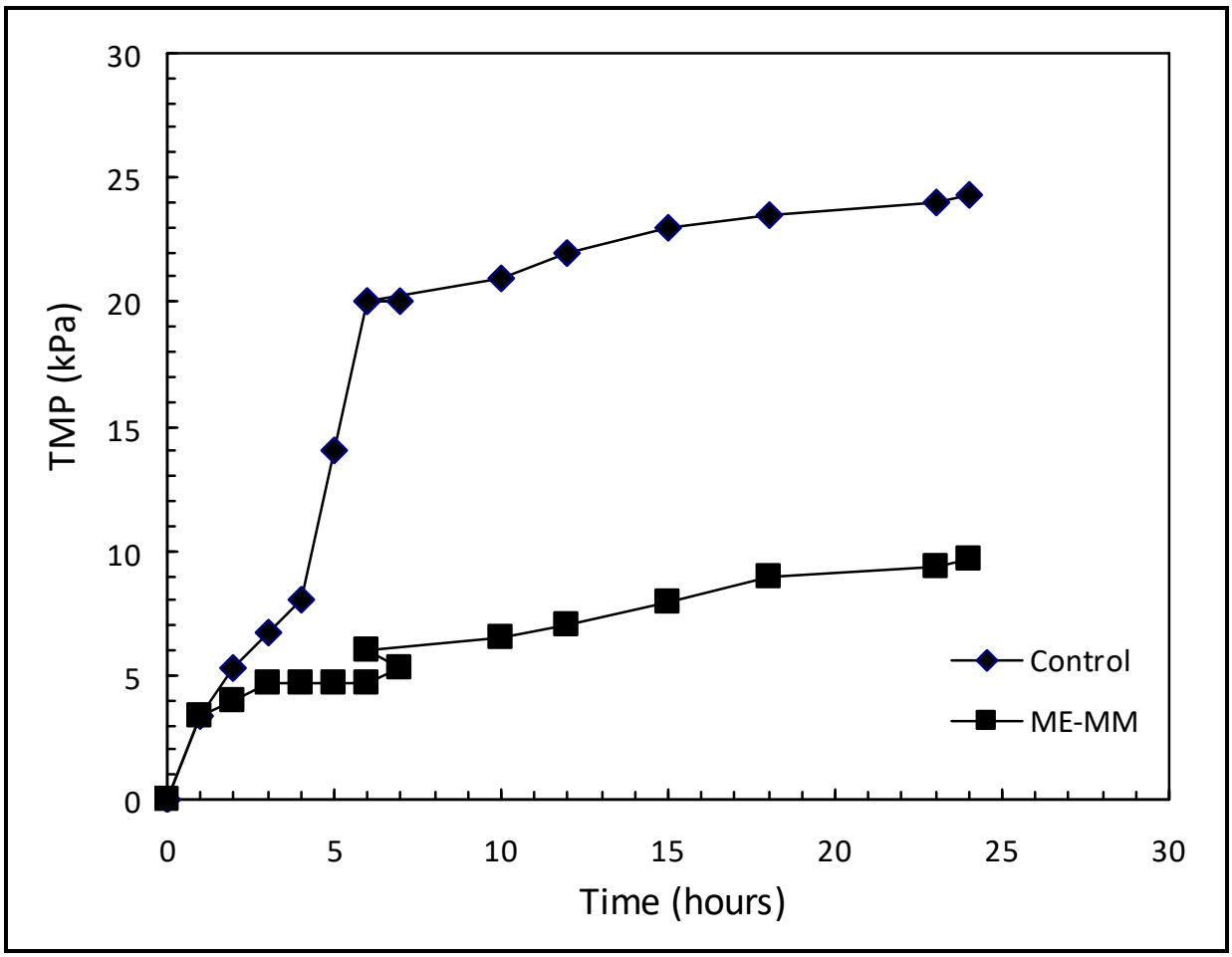

Figure 15. Investigation of the fouling reduction potential of MEMM system.

For both reactors, the TMP rose exponentially at the beginning (up to 3 hours) of filtration, due to polarization concentration and rapid foulant build-up at the membrane surfaces. After that, a continuous exponential increase of TMP occurred for control reactor. The back transport from hydrodynamic created by mechanical mixing was lower than the fouling rate resulting the severe fouling. The TMP start to rise at lower rate for the following stage, reaching 243 mbar after 24 hours of operation.

In the MEMM system, after initial exponential rose up to 3 hours from the starting the filtration, the TMP started to stabilize at a much lower TMP of 47 mbar, following by weak rise of TMP and reached a final value of 97 mbar after 24 hours of operation. After subsequent amount of foulant accumulated at membrane surface, the foulant degraded by ME facilitating the prevention of exponential rise of TMP. These results showed a preliminary indication on the effectiveness of the MEMM system to control membrane fouling. The ME in bulk attracted by mean of magnetic forces onto MM surfaces and work very locally, precisely where it required on the membrane surface. This makes MEMM system is expected to be a very efficient for fouling control. However, by the time passed the lost on the ME activity occurred resulting the slow increase of TMP.

DOI: http://dx.doi.org/10.17509/ijost.v1i1
p- ISSN 2528-1410 e- ISSN 2527-8045

4.3.3.3. Enzymatic cleaning potential of MEC

After the test of Section 4.4.2 had finished, the membranes from both systems (MEMM and control) were switched. The MM (M-1) that was placed in the MEMM system was switched with the MM (M-2) that was placed in the control system. Prior to the filtration started, M-1 was physically cleaned by using pressurized tap water to release the irreversibly attached ME from the surfaces and M-2 left in fouled condition. The profile of filtration for the test on the cleaning potential of MEMM system is shown in **Figure 16.** As expected, the initial TMP of M-2 is higher than M-1. In case of M-1, considerably high initial TMP was due to the foulant trapped inside the pores that could not be removed and for M-2 it was obviously due to the accumulated foulant from previous test. After an extension of filtration period, the TMP increased at an almost exponential rate during the first two hours and attained a value of 207 mbar after 24 hours for M-1. A different TMP behavior was obtained for M2. The TMP first decreased for the first three hours and reached a value of 153 mbar following by weak increase of TMP. The decrease of TMP just after the filtration started indicates the occurrence of enzymatic cleaning on the fouled membrane surfaces. However, the TMP of M-1 started to increase again due to a loss in ME activity but still showed better performance than the control (M-2).

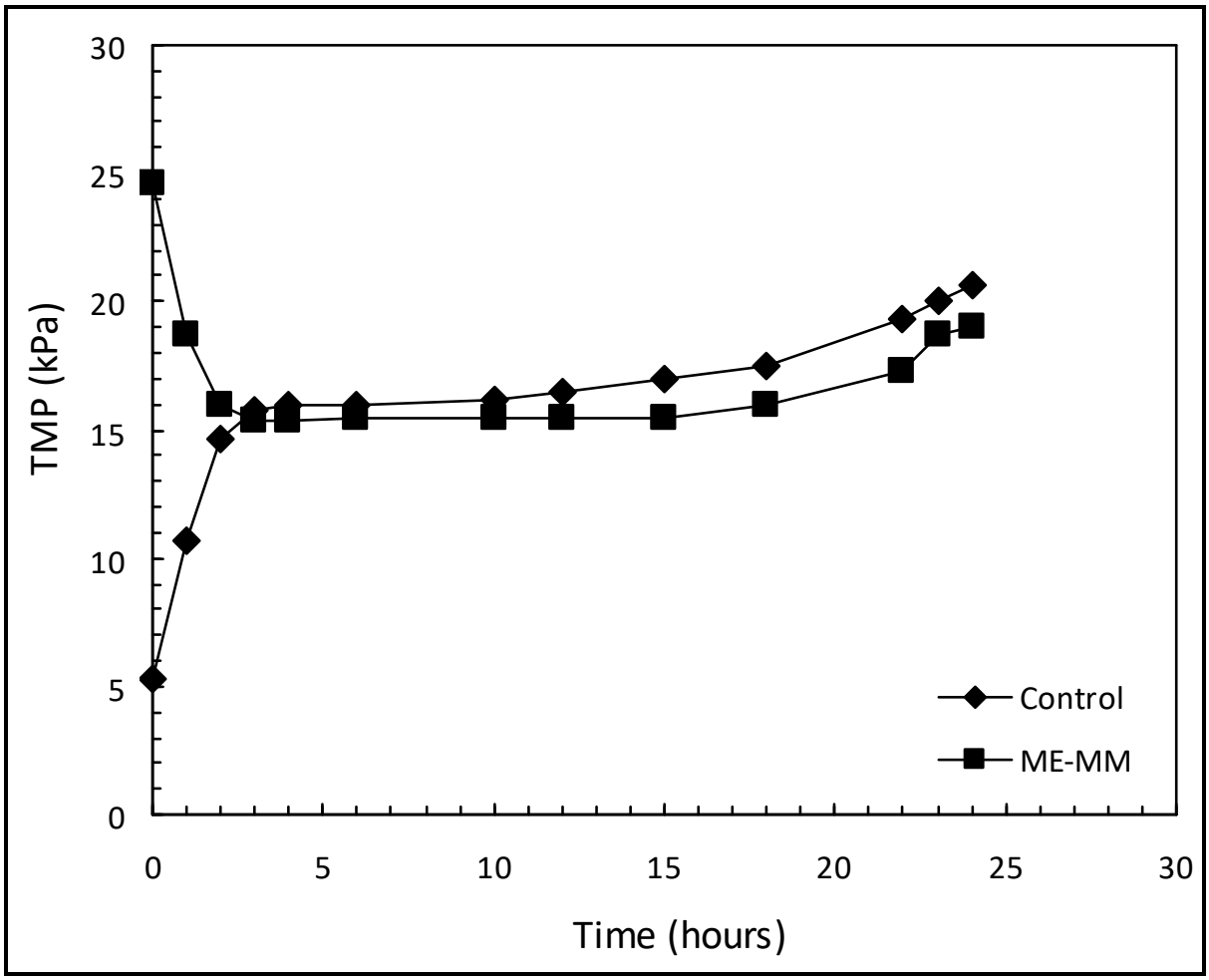

Figure 16. Investigation of the cleaning potential of MEMM

DOI: http://dx.doi.org/10.17509/ijost.v1i1
p-ISSN 2528-1410 e-ISSN 2527-8045

Overall results from system test obviously showed the effectiveness of MEMM system for controlling membrane fouling. This approach can be a potential alternative and a possible breakthrough for fouling control in MBR. However, it should be realized that enzymatic cleaning has some inherent drawbacks to some extent may limit its large scale application. The activity of enzyme is very sensitive to temperature, pH or even to elevated salt concentration. This problem should be addressed to increase the feasibility of the system to be applied in real wastewater treatment. The proper immobilization system has shown promising result in maintaining high stability of enzyme (Yeon *et al.*, 2009).

5. CONCLUSIONS

In this study, the novel MEMM system was developed and tested. The MM and ME which are main component of this system were successfully prepared and optimized. The MM has well distributed MNP on its surfaces and could be prepared by adding MNP on casting solution and introducing a sonification step on casting procedure. The properties were not significantly different compare to fresh membrane. The BsXynA has an optimum activity at a pH of 6-7 and a temperature of 40°C and stable at pH range of 3-8 and at temperatures of 20-40°C. The HPAEC-PAD analysis and FTIR were able to be used to prove the presence of coupling in ME. The optimum parameters for coupling of BsXynA onto MNP were achieved when using MNP with 10% acid groups, enzyme to NP ratio of 0.1/1, 2-hour reaction time, water as coupling medium and by storage the ME in MOPS buffer. The filtration test on the MEMM system proved the effectiveness of the system to be applied for fouling control in MBRs. However, further works are still required to implement this approach in real MBRs. The choice of immobilization technique to maintain high activity and stability of enzyme in MBRs operational conditions is an imperative. To address the fouling in MBRs, the mixture of enzymes is also need to be applied.

6. ACKNOWLEDGEMENTS

K.U. Leuven for supporting the frame of the CECAT excellence, GOA and IDO financing, and the Flemish Government for the Methusalem funding and the Federal Government for an IAP grant.

7. AUTHOR'S NOTES

The author(s) declare(s) that there is no conflict of interest regarding the publication of this article. Authors confirmed that the data and the paper are free of plagiarism.

8. REFERENCES

Bilad, M. R., Declerck, P., Piasecka, A., Vanysacker, L., Yan, X., and Vankelecom, I. F. (2011). Development and validation of a high-throughput membrane bioreactor (HT-MBR). *Journal of membrane science*, 379(1), 146-153.

Cho, B. D., and Fane, A. G. (2002). Fouling transients in nominally sub-critical flux operation of a membrane bioreactor. *Journal of membrane science*, 209(2), 391-403.

Chu, L., and Li, S. (2006). Filtration capability and operational characteristics of dynamic membrane bioreactor for municipal wastewater treatment. *Separation and purification technology*, 51(2), 173-179.

Herzberg, M., Kang, S., and Elimelech, M. (2009). Role of extracellular polymeric substances (EPS) in biofouling of reverse osmosis membranes. *Environmental science and technology*, 43(12), 4393-4398.

Hwang, B. K., Lee, W. N., Yeon, K. M., Park, P. K., Lee, C. H., Chang, I. S., Drews, A., and Kraume, M. (2008). Correlating TMP increases with microbial characteristics in the bio-cake on the membrane surface in a membrane bioreactor. *Environmental science and technology*, 42(11), 3963-3968.

Judd, S., The MBR Book (2006): *Principles and Applications of Membrane Bioreactors in Water and Wastewater Treatment* (first ed), Elsevier, Amsterdam Boston London (2006).

Le-Clech, P., Chen, V., and Fane, T. A. (2006). Fouling in membrane bioreactors used in wastewater treatment. *Journal of membrane science*, 284(1), 17-53.

Loiselle, M., and Anderson, K. W. (2003). The use of cellulase in inhibiting biofilm formation from organisms commonly found on medical implants. *Biofouling*, 19(2), 77-85.

Maartens, A., Swart, P., and Jacobs, E. P. (1996). An enzymatic approach to the cleaning of ultrafiltration membranes fouled in abattoir effluent. *Journal of membrane science*, 119(1), 9-16.

Meng, F., and Yang, F. (2007). Fouling mechanisms of deflocculated sludge, normal sludge, and bulking sludge in membrane bioreactor. *Journal of membrane science*, 305(1), 48-56.

Meng, F., Chae, S. R., Drews, A., Kraume, M., Shin, H. S., and Yang, F. (2009). Recent advances in membrane bioreactors (MBRs).: membrane fouling and membrane material. *Water research*, 43(6), 1489-1512.

Pollet, A., (2010). *Functional and structural analysis of glycosidehydrolase family 8, 10 and 11 xylanases with focus on Bacillus subtilis xylanase A.* (Ph.D. thesis, K.U.Leuven, Belgium).

Pollet, A., Beliën, T., Fierens, K., Delcour, J. A., and Courtin, C. M. (2009). Fusarium graminearum xylanases show different functional stabilities, substrate specificities and inhibition sensitivities. *Enzyme and microbial technology*, 44(4), 189-195.

Puspitasari, V. (2009). *Membrane cleaning and ageing effect by chemical and enzymatic agents.* (Master thesis, Chemical sciences and engineering, Faculty of engineering, UNSW).

Ramesh, A., Ramesh, A., Lee, D. J., and Lai, J. Y. (2007). Membrane biofouling by extracellular polymeric substances or soluble microbial products from membrane bioreactor sludge. *Applied microbiology and biotechnology*, 74(3), 699-707.

Vandermarliere, E., Bourgois, T. M., Rombouts, S., Van Campenhout, S., Volckaert, G., Strelkov, S. V., Delcour, A., Rabijns, A., and Courtin, C. M. (2008). Crystallographic analysis shows substrate binding at the 3 to+ 1 active-site subsites and at the surface of glycoside hydrolase family 11 endo-1, 4-β-xylanases. *Biochemical journal*, 410(1), 71-79.

DOI: http://dx.doi.org/10.17509/ijost.v1i1
p-ISSN 2528-1410 e-ISSN 2527-8045

Vandezande, P., Gevers, L. E., Paul, J. S., Vankelecom, I. F., and Jacobs, P. A. (2005). High throughput screening for rapid development of membranes and membrane processes. *Journal of membrane science*, 250(1), 305-310.

Vankelecom, F.J., De Smet, K., Gevers, L., Jacobs, P. (2004). Preparation of NF-membranes. In: Schäfer A., Fane A., Waite T. (Eds.), Nanofiltration - Principles and applications. *Elsevier*.

Visvanathan, C., Aim, R. B., and Parameshwaran, K. (2000). Membrane separation bioreactors for wastewater treatment. *Critical reviews in environmental science and technology*, 30(1), 1-48.

Wang, X. M., Li, X. Y., and Huang, X. (2007). Membrane fouling in a submerged membrane bioreactor (SMBR): Characterisation of the sludge cake and its high filtration resistance. *Separation and purification technology*, 52(3), 439-445.

Wang, Z., Wu, Z., Yin, X., and Tian, L. (2008). Membrane fouling in a submerged membrane bioreactor (MBR) under sub-critical flux operation: membrane foulant and gel layer characterization. *Journal of membrane science*, 325(1), 238-244.

Yeon, K. M., Lee, C. H., and Kim, J. (2009). Magnetic enzyme carrier for effective biofouling control in the membrane bioreactor based on enzymatic quorum quenching. *Environmental science and technology*, 43(19), 7403-7409.

Zhang, J., Chua, H. C., Zhou, J., and Fane, A. G. (2006). Factors affecting the membrane performance in submerged membrane bioreactors. *Journal of membrane science*, 284(1), 54-66.

DOI: http://dx.doi.org/10.17509/ijost.v1i1
p- ISSN 2528-1410 e- ISSN 2527-8045